Magnetoelastic response of $La_{0.7}Sr_{0.3}MnO_3/SrTiO_3$ superlattices to reversible strain

M. C. Dekker,[1,*] A. Herklotz,[1] L. Schultz,[1] M. Reibold,[2] K. Vogel,[2] M. D. Biegalski,[3] H. M. Christen,[3] and K. Dörr[1,4,†]

[1]*IFW Dresden, P.O.B. 270116, 01171 Dresden, Germany*

[2]*Institute for Structure Physics, Technische Universität Dresden, 01062 Dresden, Germany*

[3]*Oak Ridge National Laboratory, Center for Nanophase Materials Sciences, Oak Ridge, Tennessee 37830-6488, USA*

[4]*Institute for Physics, MLU Halle-Wittenberg, 06120 Halle, Germany*

(Received 10 December 2010; revised manuscript received 3 April 2011; published 17 August 2011)

The influence of an electrically controlled biaxial in-plane strain on the magnetization of superlattices of ferromagnetic $La_{0.7}Sr_{0.3}MnO_3$ and $SrTiO_3$ was studied for single-layer thicknesses of $d = 1.5$–13 nm. Superlattices were grown by pulsed laser deposition on both $SrTiO_3$(001) and piezoelectric $0.72Pb(Mg_{1/3}Nb_{2/3})O_3$–$0.28PbTiO_3$(001), or PMN-PT(001), substrates and have been structurally characterized by x-ray diffraction (XRD) and transmission electron microscopy. Grazing-incidence XRD reveals the vertical homogeneity of the piezoelectrically controlled reversible in-plane strain, even in a 600-nm-thick superlattice containing 100 oxide interfaces. The as-grown strain is almost identical in all superlattices that are coherently grown, with small variations resulting from the partially relaxed growth of the first $La_{0.7}Sr_{0.3}MnO_3$ layer on PMN-PT(001). The magnetic transition temperature decreases with the layer thickness d as a consequence of the finite layer thickness, and the strain-induced response of the magnetization changes its character from that of a long-range-ordered ferromagnet to that of a magnetically disordered (possibly electronically phase-separated) manganite. The strain response of a modified interface layer ("dead layer") of the thickness d_I is distinguished from that of the layer's interior by its different temperature dependence, allowing an estimation of 10 Å $< d_I <$ 16 Å for the superlattices on PMN-PT.

DOI: 10.1103/PhysRevB.84.054463 PACS number(s): 75.80.+q

I. INTRODUCTION

Superlattices (SLs) grown from complex oxide components bear the promise of creating electronic properties and functionalities that are not found in the respective bulk materials. Prominent examples are the quasi-two-dimensional metallic state at interfaces between two insulators ($LaAlO_3/SrTiO_3$),[1,2] the magnetoelectric effect arising from symmetry breaking at interfaces,[3] and the strongly enhanced ordering temperatures in solid-solution oxides whose ions have been artificially ordered by atomic-layer-wise deposition.[4] Phenomena such as magnetic exchange interactions at interfaces in SLs composed of magnetic metals have recently been observed in oxide SLs, such as antiferromagnetic[5] or perpendicular[6] coupling between adjacent magnetic layers. At the interface between a magnet and a ferroelectric, the electric control of the ferroelectric polarization allows for manipulation of the interface charge concentration and thereby the magnetic moment[7] and spin polarization[8] in the magnetic layer.

After charge concentration, lattice strain is the second central parameter governing the electronic state of complex oxides. Elastic strain may remove the orbital degeneracy, may alter exchange interactions through changes of bond angles and lengths, and has a vital influence on ferroelectric ordering (e.g., Ref. 9). SLs with coherently grown, flat layers provide a homogeneous strain state that can be tuned by the choice of substrate and interlayer materials and kept constant over much larger thicknesses than in single films. Advances in growth and characterization techniques have led to strongly improved quality of oxide SLs in recent years. Mapping of elemental distributions and valence states across interfaces by electron energy loss spectroscopy in scanning transmission electron microscopy (STEM) provides a means to detect intermixing and segregation of elements at interfaces with the resolution of a single unit cell.[10–13] X-ray scattering and x-ray absorption techniques using modern synchrotron x-ray sources have opened pathways for a sensitive detection of changes in lattice parameters and valence states, electron orbital reconstructions, and local magnetic moments at coherent oxide interfaces (e.g., Refs. 14–16). As a means of studying the influence of elastic strain on the structural,[17] electronic,[18] and optical[19] properties of materials directly, piezoelectric monocrystalline substrates of $0.72Pb(Mg_{1/3}Nb_{2/3})O_3$–$0.28PbTiO_3$(001), hereafter referred to as PMN-PT(001)[17,20–22] have been introduced.

$La_{0.7}Sr_{0.3}MnO_3$ (LSMO) is known for its very high spin polarization.[23] The magnetism of ultrathin $La_{0.7}Sr_{0.3}MnO_3$ layers has been investigated to understand the interface behavior that is vitally important for spintronics devices. SLs with $La_{0.7}Sr_{0.3}MnO_3$ and $SrTiO_3$ (STO) layers,[24–34] as well as ultrathin single films of ferromagnetic-metallic manganites $La_{0.7}A_{0.3}MnO_3$ (A = Sr or Ca) on $SrTiO_3$ substrates,[35–41] have been studied frequently, with layer thicknesses ranging from 1 unit cell (u.c.) (1 u.c. ≈ 3.9 Å) to ∼30 nm. One of the surfaces of the manganite layer is different in a single-layer film; nevertheless, results published for single films and SLs are quite similar thus far, provided the strain state is the same. The effect of the finite layer thickness has been separated from that of the global elastic strain induced by the substrate and/or the interlayers: SLs are favorable in that the lattice parameters remain fixed irrespective of the layer thickness d because of the coherent growth. Biaxial strain (both tensile and compressive) leads to a reduction of the Curie temperature (T_C) of $La_{0.7}Sr_{0.3}MnO_3$, which depends quadratically on the in-plane strain,[42–44] with Ref. 43 describing reversible strain measurements in single $La_{0.7}Sr_{0.3}MnO_3$ films. For $La_{0.7}Sr_{0.3}MnO_3/SrTiO_3$ SLs on $SrTiO_3$(001) substrates, the coherent in-plane lattice parameter is $a \approx 3.905$ Å, as adopted

from the substrate, resulting in a tensile strain of nominally 0.75% of the LSMO layers. With decreasing d below ∼5 nm (12 u.c.), T_C drops substantially, accompanied by a reduction in the saturated magnetization, and the manganite layers become insulating at a somewhat lower thickness, reflecting sample quality and the strain state.[24–29,32,35,36] The ferromagnetic double exchange interaction that couples ferromagnetic order and charge transport is clearly suppressed in the ultrathin layers. Thickness-dependent conduction data were found to agree with a model assuming a nonconducting layer at the interfaces of the LSMO layers (or at an interface and a surface for single films), which was called the "dead layer."[37,38,45] This layer is magnetically less ordered, so the magnetization drops in an interface-near layer (which may have a slightly different characteristic thickness from that of the electric dead layer). Previous work on magnetic tunnel junctions discussed the strong decrease of the tunneling magnetoresistance with temperature as a result of an interface-near electronic phase separation into ferromagnetic-metallic and insulating less-ordered clusters.[45,46] A theoretical analysis of this scenario was given by Brey.[47] Nuclear magnetic resonance[37] and ellipsometry[48] studies on Ca-doped ultrathin manganite films gave evidence for the coexistence of metallic and insulating phases.

The thickness of the dead layer (d_I) not only is important for applications, such as in spintronics, but is also a fundamentally interesting quantity that reflects intrinsic interfacial effects. In addition, it is strongly affected by defects and is thus a measure of the structural quality of interfaces. Some care must be taken when comparing the reported values in the literature, because the dead layer at each interface is half as thick as the thickness of the thickest insulating LSMO layer, whereas the thinnest metallic layer is typically reported as an upper limit for d_I in published work. In the latter sense, Huijben *et al.* found $2d_I < 5$ nm (13 u.c., which is the thinnest observed metallic layer) for $La_{0.7}Sr_{0.3}MnO_3/SrTiO_3$ on $SrTiO_3$(001),[35] and Kim *et al.* showed $2d_I < 2.7$ nm (7 u.c.).[36] These results are quite promising in the sense that the intrinsic dead layer is obviously thinner than reported in some earlier work that may have shown an enlarged d_I because of microstructural imperfections. Ma *et al.* reported on LSMO/STO grown on $SrTiO_3$(110),[32] which gives a higher packing density of atoms and thus a lower thickness of $2d_I < 2.0$ nm. Strained ultrathin LSMO layers were found to have a different lattice symmetry (orthorhombic,[26] as compared to rhombohedral in bulk) or show a non-bulklike orbital order,[35,49] but these results are not yet fully consistent. This may be partly because of a varied microstructure of the studied interfaces. Several authors found a segregation of Sr at the upper surface of LSMO layers.[13,14] A STEM investigation by Fitting-Kourkoutis *et al.*[13] revealed an increasing Sr segregation and intermixing at interfaces with increasing laser fluence for SLs grown by pulsed-laser deposition. For the smallest laser fluence, $2d_I < 2.0$ nm (5 u.c.) for the (001)-oriented film could be reached.[13]

In this paper, we discuss the structural and magnetic properties of LSMO/STO SLs grown on piezoelectric PMN-PT(001) substrates. The transfer of the reversibly applied strain to SLs, including one with a total thickness of 600 nm and 100 interfaces, is investigated using grazing-incidence x-ray diffraction (XRD). Reversible strain control by means of piezoelectric substrates is shown to work well in coherently grown SLs. The structure and microstructure of the LSMO/STO SLs on PMN-PT are analyzed by XRD and transmission electron microscopy (TEM). We find a slightly reduced structural quality on PMN-PT when simultaneously grown SLs on STO and PMN-PT are compared. Coherence of the SLs on PMN-PT starts from the first-grown LSMO layer. The thickness dependence $T_C(d)$ observed on PMN-PT is comparable with published data for SLs on STO substrates. With decreasing d, the strain-induced response of the magnetization of SLs on PMN-PT changes its character from that of a long-range-ordered ferromagnetic manganite to that of a magnetically disordered (and possibly electronically phase-separated) manganite. The strain response of the interface layer (dead layer) can be distinguished from that of the layer's ferromagnetic interior by its distinct temperature dependence, leading to an estimation of the thickness of the magnetically dead layer of 16 Å > d_I > 10 Å for the SLs on PMN-PT.

II. EXPERIMENT

$[La_{0.7}Sr_{0.3}MnO_3/SrTiO_3]_n$ SLs were grown by *off-axis* pulsed laser deposition[50] from stoichiometric targets of $La_{0.7}Sr_{0.3}MnO_3$ and $SrTiO_3$ on monocrystalline mixed-terminated $SrTiO_3$ (001) and PMN-PT (001) substrates simultaneously. The films were deposited in an oxygen pressure of 0.3 mbar at a substrate temperature of 700 °C with a pulse frequency of 3 Hz and cooled down in an oxygen atmosphere of 0.8 bar. Equal pulse numbers were used for both components. Two sample series were grown: series I with fixed layer thickness ($d = 4.4$ nm) and varied total thickness D, and series II with fixed total thickness $D \approx 200$ nm and $d = 1.5$–13.4 nm (∼4–33 u.c.). The deposition started with the LSMO layer and stopped with a top STO layer.

Structural characterization of SL samples was carried out by XRD using a high-resolution four-circle PANalytical X'Pert Pro MRD, a Philips X'Pert MRD (Cu Kα radiation) as well as a Siemens D5000 (Co Kα) diffractometer. In-plane lattice parameters and coherent growth were evaluated from reciprocal space mapping. Grazing-incidence measurements were employed to evaluate the changes of the in-plane lattice parameters of films and substrate upon application of the piezoelectric substrate strain, as described in Ref. 17 and later in this paper. For TEM, thin cross sections were prepared by mechanical grinding, mechanical dimpling, and etching by ion milling. The investigations were performed with a FEI Tecnai F20/Cs-corrected transmission electron microscope.

To carry out the strain-dependent measurements, the inverse piezoelectric effect of the PMN-PT substrates is used to provide an electrically controllable reversible biaxial in-plane strain.[17,43] A voltage is applied along the substrate normal using a silver paint contact on top of the SL and a NiCr/Au electrode on the bottom face of the PMN-PT crystal, producing an electric field of $E \leqslant 15$ kV/cm in the 0.3-mm-thick substrate. The large resistivity of the substrate (>10^{10} Ωcm) guarantees the correct function of the SL as an upper electrode, because its own resistivity is many orders of magnitude smaller. The resulting current is <10^{-7} A after proper poling of the crystal. The PMN-PT substrate shrinks approximately

linearly with increasing E in both in-plane directions and provides sufficiently uniform strain for quantitative studies of strain dependences, irrespective of its actual ferroelectric domain configuration (see Ref. 17 for a detailed discussion). $E = 10$ kV/cm leads to an in-plane compression of $\varepsilon = -0.11\% \pm 0.01\%$ at 300 K.[17,43] The temperature dependence of the piezoelectric substrate strain is rather weak between ~70 K and ~250 K, with an upturn above 250 K attributed to the proximity of the monoclinic-to-tetragonal phase transition and a downturn below 50 K.[22] Room temperature strains were used as approximate values for the full temperature range investigated here, leading to small overestimations of the strain for $T \geqslant 80$ K and increasingly larger overestimations for lower temperatures (reaching about a factor of 2 for the lowest temperature of 30 K). This, however, does not significantly affect the obtained results.

Magnetization measurements were carried out in a Superconducting quantum interference device (SQUID) magnetometer (Quantum Design). The sample holder is equipped with twisted Cu wires (60 μm) for the voltage supply of the substrate. The magnetization of the SL is normalized to the volume of the LSMO layers. A Curie temperature was assigned to all samples irrespective of the nature of their magnetic ordering (collinear ferromagnetic or more disordered), because the temperature where the extrapolation of the linear part of $M^2(T)$ measured during warming in a field of 100 mT crosses the T-axis (Curie-Weiss method). Breakdown of the He atmosphere in the cryostat hindered the application of $E \geqslant 10$ kV/cm below 30 K, limiting the temperature range for strain-dependent magnetization measurements.

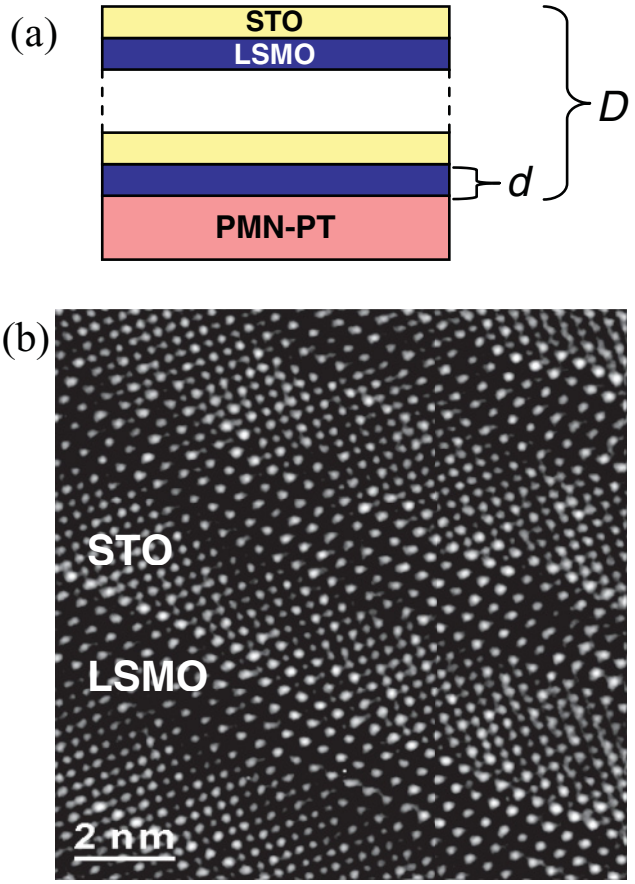

FIG. 1. (Color online) (a) $La_{0.7}Sr_{0.3}MnO_3/SrTiO_3$ SLs with total thickness D and $La_{0.7}Sr_{0.3}MnO_3$ layer thickness d. (b) Cross section of a coherent SL observed by high-resolution TEM.

III. RESULTS

A. Structure and reversible strain of the SLs

Figure 1(a) shows a schematic picture of the SLs that consist of LSMO and STO layers, beginning with a LSMO bottom layer and ending with a STO top layer. The layer thickness d refers to the thickness of the LSMO layers. High-resolution TEM images indicate coherent growth within the SLs (Fig. 1(b)) whose components have a nominal lattice misfit of 0.75%. Bulk pseudocubic lattice parameters are $a = 3.876$ Å for LSMO and $a = 3.905$ Å for STO. On PMN-PT substrates, the first LSMO layer forms dislocations because of the large nominal misfit of 3.7%.[21] The SL itself is coherent, i.e., on PMN-PT, the coherent growth starts after the first LSMO layer has been grown. The interfaces on PMN-PT show roughness of 1–2 u.c. in TEM images that may be a consequence of the slightly enhanced surface roughness of the PMN-PT compared to the STO substrates. Interfaces of SLs on STO substrates grown under the same conditions were investigated by electron energy loss spectroscopy in a previous work,[12] revealing atomically abrupt interfaces, but with the occasional occurrence of steps that are 1–2 u.c. in height, a detectable Mn valence reduction by 0.16 ± 0.10, as well as an elongation of (001) plane spacing at interfaces.

All samples show only 00l reflections in the Bragg-Brentano (Θ–2Θ) x-ray scans. The 00l peaks have several satellites from the SL reflections (Fig. 2(a)). The position of the 001 main peak is essentially independent of d, in agreement with the unchanged lattice parameters for coherent growth. The small deviations for the films on PMN-PT are a result of (1) the partially relaxed growth of the first LSMO layer on PMN-PT that leads to some scattering in the lattice parameter among different SL samples and (2) a slight variation of the substrate lattice parameters among individual PMN-PT crystals that may result from small compositional variations. Because the first LSMO layer grows with dislocations on the PMN-PT substrate, the strain state of this first layer is not fully identical among the samples, although this first layer determines the in-plane parameter for the SL. The SL period $\Lambda = d + d_{STO}$ has been calculated from the positions of the satellites in wide-angle Θ–2Θ x-ray measurements. The value of d is derived as $d = \Lambda \cdot 0.41$, with the factor $f = 0.41 \pm 0.02$ being the ratio of $d / (d + d_{STO})$. f has been determined by averaging measurements of layer thicknesses in 20 high-resolution TEM images obtained from samples with $d > 3$ nm. X-ray reflectivity shows clear Kiessig oscillations, as well as the larger interference maxima from the SL peaks, giving qualitative proof of a well-defined SL structure with sharp interfaces on STO. The SLs on PMN-PT also show these reflectivity oscillations, although they are somewhat less pronounced, indicating a larger roughness (Fig. 2(b)). Reciprocal space maps around the 103 reflection (not shown in a figure) reveal a slightly larger tensile strain in the SLs on PMN-PT: the pseudotetragonal lattice parameters are $a =$

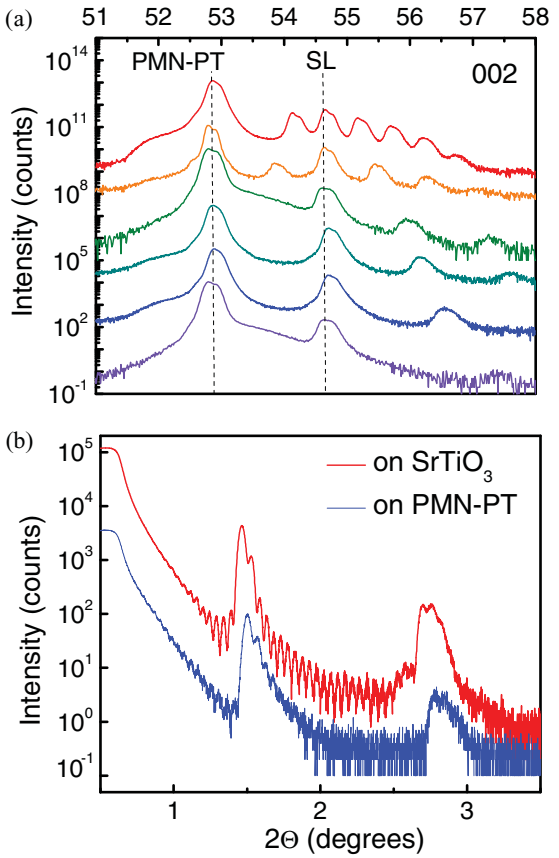

FIG. 2. (Color online) (a) X-ray Θ–2Θ diffraction pattern around the 002 peak of SLs on PMN-PT substrates with single-layer thicknesses of d = 7.9, 5.1, 3.2, 2.9, 2.1, and 1.5 nm (from series II). (b) X-ray reflectivity curves of a SL on $SrTiO_3$ (d = 3.2 nm, red curve) and a SL on PMN-PT (d = 2.7 nm, blue curve). Curves are vertically displaced for clarity.

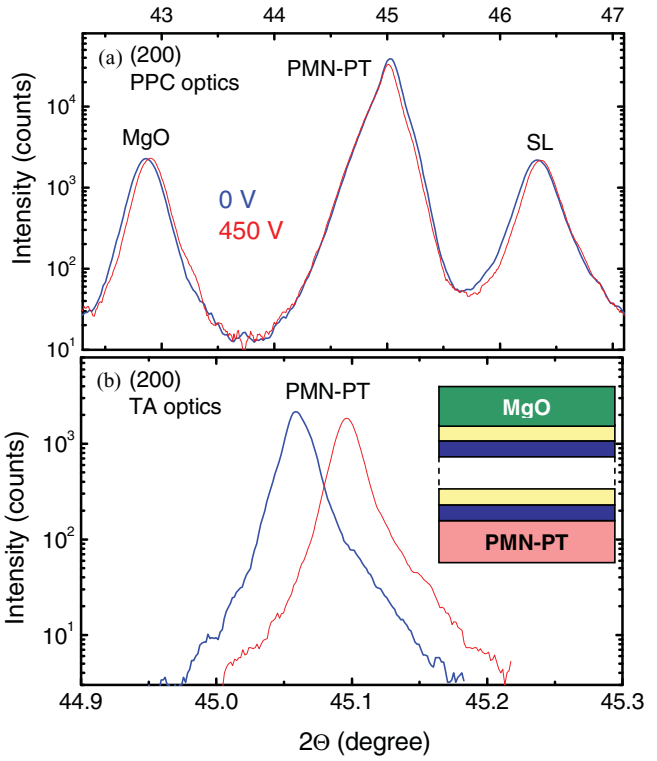

FIG. 3. (Color online) (a) Grazing-incidence XRD pattern around the 200 peak of a MgO/SL(600 nm)/PMN-PT sample (inset of (b)) in two controlled strain states with substrate voltages of 0 V (thick blue line) and 450 V (thinner red line). The narrow substrate peak is not properly resolved using the PPC detector optics applied in (a). (b) The substrate peak has been measured correctly using a triple-axis (TA) detector.

3.912 and 3.905 Å (in plane) and c = 3.901 and 3.906 Å) (out of plane) on PMN-PT and STO, respectively. Thus, LSMO layers are under larger tensile strain of nominally 0.95% with respect to the bulk lattice parameter in the SLs on PMN-PT than in those on STO (0.75%).

The changes of lattice parameters (a and c) of both the SL and the substrate upon the application of an electrically controlled reversible substrate strain have been investigated by XRD for several samples. Thicker SLs (D > 300 nm) were deposited only on part of the substrate area to leave direct access to the substrate for recording sufficient substrate peak intensities. In addition, a MgO film was deposited on top of the SL as a strain indicator. Because MgO has a larger lattice parameter (4.20 Å), the MgO film peaks are easily discernible and directly reflect the amount of strain transferred through the SL. In Fig. 3, the 200 in-plane reflections of the MgO top layer, a SL with d = 6 nm / D = 600 nm and the substrate are shown for two applied substrate voltages (0 and 450 V) leading to an applied field of 0 or 15 kV/cm. The approximately equal right shift of the reflections from the SL and the MgO top layer revealing the in-plane compression upon voltage application. However, while a parallel-plate collimator (PPC) (Fig. 3(a)) yields accurate results for the rather wide film peaks, the narrower substrate peak had to be measured using a triple-axis detector (Fig. 3(b)) to obtain the correct strain shift. The PPC optics significantly distorted the shape of this much narrower peak (full width at half maximum of ∼0.02°), yielding incorrect strain values. Fitting of the peak positions of several in-plane reflections was carried out to estimate the in-plane strain $\varepsilon = [a(E) - (E = 0)] / a(E = 0)$ for the substrate, the SL, and the MgO layer. The obtained strain values are equal within the experimental error of ±0.01%. This result shows that the elastic in-plane strain was completely transferred to the top MgO layer through the 600-nm-thick SL that contains 100 coherent oxide interfaces. Similar measurements on other SLs support this finding. (The grazing-incidence measurement of the substrate is tricky because of the necessity of avoiding scattering from the substrate sides that may contain a less strained surface layer because of their roughness.) The observation suggests that no plastic strain relaxation processes take place in the straining of this oxide SL at 300 K at the applied time scale of about an hour. The SL responds to the substrate strain coherently, much like a single crystal. Furthermore, those interfaces containing dislocations (LSMO/PMN-PT and MgO/STO) are fully transferred the elastic strain.

B. Strain-dependent magnetization

The magnetic ordering temperature (T_C) is known to decrease with reduced thickness of the LSMO layers as a

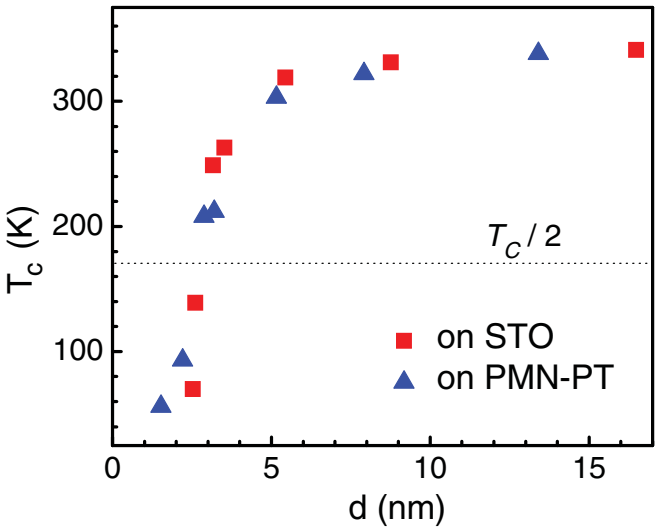

FIG. 4. (Color online) Curie temperature recorded in a magnetic field of $\mu_0 H = 0.1$ T vs thickness of the $La_{0.7}Sr_{0.3}MnO_3$ layers for SLs on STO(001) (quadratic symbols) and PMN-PT(001) (triangles), respectively.

consequence of the finite extension in the third dimension.[35,36] In Fig. 4, T_C of the SL series on STO and PMN-PT substrates is plotted as a function of the LSMO layer thickness. (Recall that T_C has been specified as the onset temperature of magnetization, as described in the Experiment section, irrespective of the type of collinear or reduced magnetic order.) The strong drop of T_C below $d = 5$ nm is in agreement with earlier observations, as is layers of $d > 10$ nm reaching a nearly bulklike value of T_C. The latter (340 K) is suppressed with respect to the single-crystal value (370 K) as a consequence of the tensile strain (0.75% and 0.95% for STO and PMN-PT, respectively). The slightly larger tensile strain of the LSMO layers on PMN-PT has an influence on T_C that is below the scattering of the measured values. The growth rate on both substrates was systematically different, so no SLs with equal values of d could be compared. The onset of magnetic order for low values of d is rather comparable in the SLs on PMN-PT and on STO. It is interesting to compare literature data with respect to the drop of $T_C(d)$ at low thicknesses: all work[25,29,32,35,36] cited here that report an explicit $T_C(d)$ dependence for the same composition, orientation, and strain of LSMO found a reduction of T_C by 50% at $d = 2$–2.5 nm (5–6 u.c.). This value also is observed in the present work (Fig. 4, $d(T_C/2) = 2.5$ nm).

The relative change in the magnetization $\Delta M/M_{V=0} = (M(V) - M_{V=0}) / M_{V=0}$ (with $M_{V=0}$ as the value measured at $V = 0$) resulting from the biaxial substrate compression under the applied voltage V has been measured in dependence on temperature. A biaxial strain $\varepsilon \approx -0.11\%$ is obtained for $V = 300$ V. Figure 5 compares the temperature dependences of $M(T)$ and $\Delta M/M_{V=0}(T)$ in three SLs with varied total SL thickness: $d = 4.4$ nm and $D = 55.5$, 111, and 234 nm. The two thicker SLs show an identical strain response $\Delta M/M_{V=0}$ within the experimental error. This is in agreement with both SLs having the same as-grown lattice parameters/strain state and the reversible strain being completely transferred through the SL irrespective of the thickness D. The larger

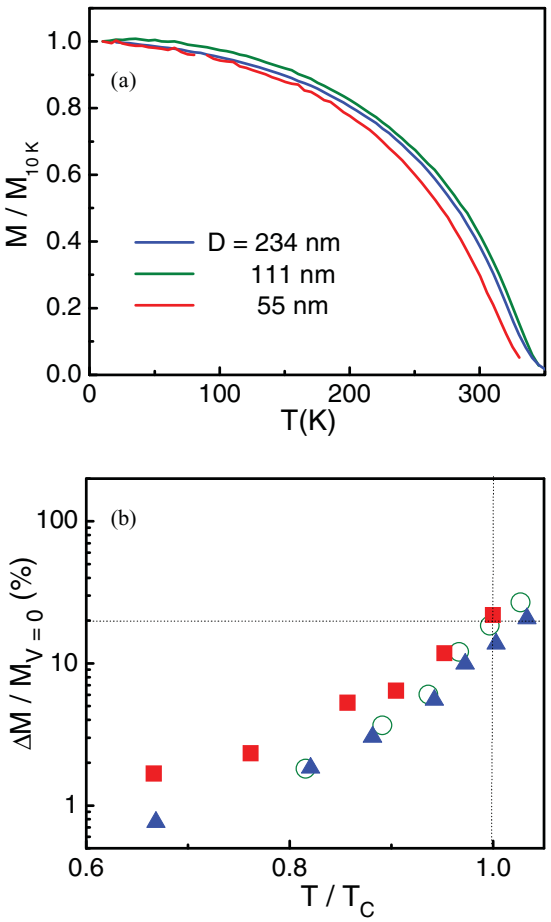

FIG. 5. (Color online) Temperature dependences of (a) the magnetization (M) normalized to the value at 10 K and (b) the magnetoelastic response $\Delta M/M$ normalized to the value obtained for the substrate voltage $V = 0$, both recorded for $\mu_0 H$ // 100 = 0.1 T. Three samples are shown with total thickness $D = 55$, 111, and 234 nm for a layer thickness of $d = 4.4$ nm (series I).

strain response of the 55.5 nm SL (Fig. 5(b)) is attributed to its slightly larger tensile strain in the as-grown state that is reflected by the somewhat lower T_C. (The strain response of a double exchange ferromagnet is not linear but quadratic,[42,43] leading to a larger response at larger as-grown tensile strain.) A magnetoelastic response of $\Delta M/M_{V=0} \approx 20\%$ is found near $T / T_C = 1$, with a continuous drop occurring with decreasing temperature (Fig. 5). (The way T_C is determined gives finite values of M also somewhat above T_C, but the determined values of $\Delta M/M_{V=0}$ have an increasingly large error.) For thicker single films of LSMO, the maximum strain response is well known to occur around T_C.[21,43] It originates from a strain-induced change of the exchange interactions that have a large effect on M near T_C and a negligible effect at $T < T_C$, where ferromagnetic order is established. The piezoelectric biaxial compression releases part of the as-grown tensile strain in the LSMO layers, the unit cells lose part of their tensile distortion, and thus, ferromagnetic double exchange interactions are enhanced. The detailed microscopic nature of the unit cell distortions with respect to changes of bond angles and lengths is yet to be explored. For instance, it might be accessible by a recently introduced approach to measure

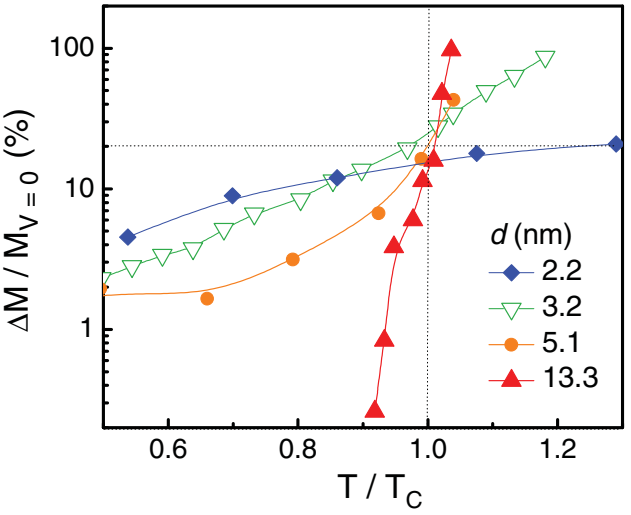

FIG. 6. (Color online) Magnetoelastic response (determined as in Fig. 5 (b)) vs normalized temperature for four manganite layer thicknesses d (sample series II).

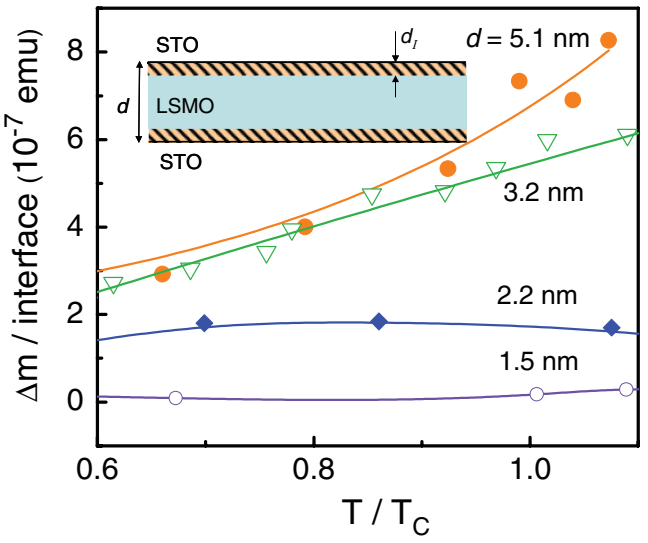

FIG. 7. (Color online) Strain-induced change in the magnetic moment per interface for SLs of series II with the indicated layer thicknesses. The inset shows a model of the manganite layers containing a nonferromagnetic ("dead") layer of thickness d_I at each interface with the STO layers.

collective rotations and distortions of the oxygen octahedra by synchrotron-based XRD.[51]

The influence of the manganite layer thickness d can be seen in the examples plotted in Fig. 6. The quasisaturated magnetization measured at 5 T and 10 K decreases by about a factor of 4 between $d = 13.4$ and 1.5 nm, revealing the loss of magnetic order with reduced layer thickness. A steep temperature dependence of the strain response $\Delta M/M_{V=0}$ is found for the SL with the thickest layers ($d = 13.4$ nm). It drops to a value below the measurable limit ($< 0.1\%$) at $T \leqslant 0.9\ T_C$. This suggests that the magnetic order (parallel alignment of the Mn spins) in the bulk of the thick LSMO layers is quite complete at lower temperatures, because it is insensitive to an enhancement of the ferromagnetic exchange. This observation is in agreement with earlier measurements on bulklike LSMO films.[43] Interestingly, the strain response at T_C is quite equal for all SLs irrespective of d, $\Delta M/M_{v=0}$ ($T = T_C$, $\varepsilon = -0.1\%$) $= 20\% \pm 5\%$. This value is also similar for thicker single films of LSMO under the condition of a comparable as-grown strain state.[43] Thus, the value seems to reflect an intrinsic strain response at T_C for the given as-grown tensile strain. Because M is not a particularly defect-sensitive property (e.g., as compared to electric conduction), the observation of an intrinsic strain response in various samples seems reasonable and shows the reproducibility of the magnetoelastic response. With decreasing d, the low-temperature value of $\Delta M/M_{V=0}$ increases systematically and substantially. For the smaller d, $\Delta M/M_{V=0} = 1\%$–5% at $T = 30$ K, i.e., the strain response remains notable at low temperatures. Thus, tensile strain suppresses the magnetic order in SLs with small d at $T < T_C$. This may have two origins: (1) the modified magnetic state at interfaces that becomes noticeable when the interface layers contain a sufficient fraction of the layer volume and (2) the reduced ferromagnetic order in the bulk of the layers because of their finite thickness. Without a depth-sensitive magnetic measurement (e.g., taken by neutron reflectivity), these effects are hard to separate. However, based on the accepted state of knowledge in this type of SL, we assume the interface effect (origin 1) to be dominating. Interestingly, a comparable temperature dependence of the strain response, $\Delta M/M_{v=0}(T)$, has been found in 100-nm-thick films of $(Pr_{0.4}La_{0.6})_{0.7}Ca_{0.3}MnO_3$, where it has been related to the phase-separated nature of this manganite.[52] The reversible strain has been suggested to influence the magnetic phase coexistence, with the release of tensile strain favoring the ferromagnetic-metallic state.[52] Such a phase-separated state has been suggested to exist at the interfaces of ferromagnetic-metallic manganites with insulating tunnel barriers.[45–47] The microscopic magnetic nature of the interface region in the present SLs cannot be identified here, but the similarity of both results is consistent with an electronic phase separation at the interfaces.

We have considered a simple model of the distribution of magnetic order in the LSMO layers (inset of Fig. 7) comprising an internal layer with collinear ferromagnetic order and two interface layers of fixed thickness d_I. For this model, we expect a strain response from the interfaces that is independent of d for $d > 2d_I$. At low temperatures, this interface response strongly dominates over the negligible contribution from the ordered internal layer. Therefore, we investigated the strain-induced change of the absolute magnetic moment of the SLs with small d per interface (Fig. 7). The two SLs with $d = 5.1$ and 3.2 nm indeed approximately fulfill the condition of equal values at low temperatures. In contrast, the next-thinner SLs ($d = 2.2$ and 1.5 nm) reveal a strong drop of the strain-induced magnetization per interface at low temperatures. This indicates that no ferromagnetic internal part is left in these thinnest LSMO layers, and the interface layers are reduced in thickness. In this way, we can estimate the thickness d_I as $1.0\,\text{nm} < d_I < 1.6\,\text{nm}$ (3–4 u.c.). This value of d_I is comparable to the lowest values derived from electric measurements.[13,36] Considering both the thickness dependence of T_C and this result, the interface quality of the present SLs on PMN-PT

substrates appears to be only slightly inferior in comparison to simultaneously grown SLs on STO substrates.

IV. CONCLUSIONS

The presented structural and magnetic data reveal that coherent SLs of $La_{0.7}Sr_{0.3}MnO_3/SrTiO_3$ can be grown with good structural quality on piezoelectric PMN-PT(001) substrates. XRD demonstrates that reversible uniform biaxial in-plane strain of $\leqslant 0.11\%$ has been applied to the SLs and is homogeneously transferred, even through a 600-nm-thick SL with 100 interfaces. This result indicates the fully elastic nature of the strain response of an epitaxial oxide heterostructures at $T \leqslant 300$ K, which is a prerequisite for the study of strain effects at oxide interfaces. Magnetization measurements on the SLs show the well-known suppression of ferromagnetic ordering with decreasing thickness of the LSMO layers and the suppressed ferromagnetism at the interfaces. No significant difference in magnetic ordering/magnetization was found between the SLs simultaneously grown on $SrTiO_3$ and on PMN-PT substrates, indicating comparably good structural quality. The reduction of T_C with decreasing layer thickness agrees with published data, giving 50% of the value of the thick-film limit at $d \approx 2.5$ nm (6 u.c.). The temperature dependence of the strain response of the magnetization changes with decreasing layer thickness and resembles that of phase-separated $(Pr_{0.4}La_{0.6})_{0.7}Ca_{0.3}MnO_3$ films for layer thicknesses below 4 nm. The magnetic strain response of the interfaces can be distinguished from that of the bulk of the layers based on its different temperature dependence. The magnetoelastic response of the interfaces starts to drop below a film thickness of 3.2 nm, indicating a thickness of the magnetic interface layer below 1.6 nm. In addition to clarifying the magnetic properties of epitaxial $La_{0.7}Sr_{0.3}MnO_3/SrTiO_3$ SLs under biaxial strain, our results further demonstrate that the total thickness of the uniformly strained SLs can be as large as 600 nm, making them appropriate, for instance, for neutron diffraction under reversibly controlled strain. The remaining limiting factor for a wider utilization of the PMN-PT substrates is the reduced surface quality compared to other monocrystalline oxide substrates. PMN-PT's ferroelectric domains will have a similar effect as the rhombohedral domains in the widely used $LaAlO_3(001)$ substrate that has a comparable rhombohedral distortion.[17] Optimizing buffer layers may help to improve this situation. A buffer layer system that allows for the adjustment of the in-plane lattice parameter between 3.79 and 4.05 Å to enable various as-grown strain states of films on PMN-PT has been developed recently.[53]

ACKNOWLEDGMENTS

This work has been supported by the Deutsche Forschungsgemeinschaft, Forschergruppe FOR 520 *Ferroic Functional Elements* "Ferroic Functional Elements." The portion of the research conducted at the Center for Nanophase Materials Sciences was sponsored by the Scientific User Facilities Division of the US Department of Energy.

*Present address: Max-Planck Institute for Microstructure Physics, Weinberg 2, D-06120 Halle, Germany.
†kathrin.doerr@physik.uni-halle.de

[1] R. Pentcheva and W. E. Pickett, J. Phys. Cond. Matter **22**, 043001 (2010).
[2] A. Ohtomo and H. Y. Hwang, Nature **427**, 423 (2004).
[3] N. Kida, H. Yamada, H. Sato, T. Arima, M. Kawasaki, H. Akoh, and Y. Tokura, Phys. Rev. Lett. **99**, 197404 (2007).
[4] S. J. May *et al*., Nat. Mat. **8**, 892 (2009).
[5] M. Ziese *et al*., Phys. Rev. Lett. **104**, 167203 (2010).
[6] Y. Takamura, F. Yang, N. Kemik, E. Arenholz, M. D. Biegalski, and H. M. Christen, Phys. Rev. B **80**, R180417 (2009).
[7] H. J. A. Molegraaf, J. Hoffman, C. A. F. Vaz, S. Gariglio, D. van der Marel, C. H. Ahn, and J.-M. Triscone, Adv. Mat. **21**, 3470 (2009).
[8] V. Garcia *et al*., Science **327**, 1106 (2010).
[9] H. N. Lee, H. M. Christen, M. F. Chisholm, C. M. Rouleau, and D. H. Lowndes, Nature **433**, 395 (2005).
[10] F. Pailloux, D. Imhoff, T. Sikora, A. Barthelemy, J. L. Maurice, J. P. Contour, C. Colliex, and A. Fert, Phys. Rev. B **66**, 014417 (2002).
[11] D. A. Muller, L. Fitting-Kourkoutis, M. Murfitt, J. H. Song, H. Y. Hwang, J. Silcox, N. Dellby, and O. L. Krivanek, Science **319**, 1073 (2008).
[12] T. Riedl, T. Gemming, K. Dörr, M. Luysberg, and K. Wetzig, Microsc. Microanal. **15**, 213 (2009).
[13] L. Fitting-Kourkoutis, J. H. Song, H. Y. Hwang, and D. A. Muller, PNAS **107**, 11682 (2010).
[14] R. Herger *et al*., Phys. Rev. B **77**, 085401 (2008).
[15] J. Hoppler *et al*., Nat. Mat. **8**, 315 (2009).
[16] J. Chakhalian, J. W. Freeland, H.-U. Habermeier, G. Cristiani, G. Khaliullin, M. van Veenendaal, and B. Keimer, Science **318**, 1114 (2007).
[17] M. D. Biegalski, D.-H. Kim, K. Dörr, and H. M. Christen, Appl. Phys. Lett. **96**, 151905 (2010).
[18] A. D. Rata, A. Herklotz, K. Nenkov, L. Schultz, and K. Dorr, Phys. Rev. Lett. **100**, 076401 (2008).
[19] F. Ding *et al*., Phys. Rev. Lett. **104**, 067405 (2010).
[20] S. E. Park and T. R. Shrout, J. Appl. Phys. **82**, 1804 (1997).
[21] K. Dörr *et al*., Eur. Phys. J. B **71**, 361 (2009).
[22] A. Herklotz, J. D. Plumhof, A. Rastelli, O. G. Schmidt, L. Schultz, and K. Dörr, J. Appl. Phys. **108**, 094101 (2010).
[23] M. Bowen, M. Bibes, A. Barthélémy, J.-P. Contour, A. Anane, Y. Lemaître, and A. Fert, Appl. Phys. Lett. **82**, 233 (2003).
[24] M. Izumi,Y. Ogimoto, Y. Okimoto, T. Manako, P. Ahmet, K. Nakajima, T. Chikyow, M. Kawasaki, and Y. Tokura, Phys. Rev. B **64**, 064429 (2001).
[25] M. Izumi, Y. Ogimoto, T. Manako, M. Kawasaki, and Y. Tokura, J. Phys. Soc. Jap. **71**, 2621 (2002).
[26] J. Kreisel, G. Lucazeau, C. Dubourdieu, M. Rosina, and F. Weiss, J. Phys. Cond. Matt. **14**, 5201 (2002).
[27] M. Rosina, M. Audier, C. Dubourdieu, K. Fröhlich, and F. Weiss, J. Cryst. Growth **259**, 358 (2003).
[28] K. Dörr, T. Walter, M. Sahana, K.-H. Müller, K. Nenkov, K. Brand, and L. Schultz, J. Appl. Phys. **89**, 6973 (2001).

[29]M. Sahana, T. Walter, K. Dörr, K.-H. Müller, D. Eckert, and K. Brand, J. Appl. Phys. **89** 6834 (2001).
[30]L. M. Wang, J.-K. Lin, and J.-P. Shyu, Phys. Rev. B **74**, 184412 (2006).
[31]L. M. Wang, Phys. Rev. Lett. **96**, 077203 (2006).
[32]J. X. Ma, X. F. Liu, T. Lin, G. Y. Gao, J. P. Zhang, W. B. Wu, X. G. Li, and J. Shi, Phys. Rev. B **79**, 174424 (2009).
[33]Y. F. Lu, J. Klein, F. Herbstritt, J. B. Philipp, A. Marx, and R. Gross, Phys. Rev. B **73**, 184406 (2006).
[34]E. Arenholz, G. van der Laan, F. Yang, N. Kemik, M. D. Biegalski, H. M. Christen, and Y. Takamura, Appl. Phys. Lett. **94**, 072503 (2009).
[35]M. Huijben, L. W. Martin, Y.-H. Chu, M. B. Holcomb, P. Yu, G. Rijnders, D. H. A. Blank, and R. Ramesh, Phys. Rev. B **78**, 094413 (2008).
[36]B. Kim, D. Kwon, J. H. Song, Y. Hikita, B. G. Kim, and H. Y. Hwang, Sol. State Comm. **150**, 598 (2010).
[37]M. Bibes, S. Valencia, Ll. Balcells, B. Martinez, J. Fontcuberta, M. Wojcik, S. Nadolski, and E. Jedryka, Phys. Rev. B **66**, 134416 (2002).
[38]R. P. Borges, W. Guichard, J. G. Lunney, J. M. D. Coey, and F. Ott, J. Appl. Phys. **89**, 3868 (2001).
[39]M. Angeloni, G. Balestrino, N. G. Boggio, P. G. Medaglia, P. Orgiani, and A. Tebano, J. Appl. Phys. **96**, 6387 (2004).
[40]T. Walter, K. Dörr, K. -H. Müller, D. Eckert, K. Nenkov, M. Hecker, M. Lehmann, and L. Schultz, J. Magn. Magn. Mater. **222**, 175 (2000).
[41]M. Ziese, H. C. Semmelhack, K. H. Han, S. P. Sena, and H. J. Blythe, J. Appl. Phys. **91**, 9930 (2002).
[42]A. J. Millis, T. Darling, and A. Migliori, J. Appl. Phys. **83**, 1588 (1998).
[43]C. Thiele, K. Dörr, O. Bilani, J. Rödel, and L. Schultz, Phys. Rev. B **75**, 054408 (2007).
[44]C. Adamo, X. Ke, H. Q. Wang, H. L. Xin, T. Heeg, M. E. Hawley, W. Zander, J. Schubert, P. Schiffer, D. A. Muller, L. Maritato, and D. G. Schlom, Appl. Phys. Lett. **95**, 112504 (2009).
[45]J. Z. Sun, D. W. Abraham, R. A. Rao, and C. B. Eom, Appl. Phys. Lett. **74**, 3017 (1999).
[46]M.-H. Jo, N. D. Mathur, N. K. Todd, and M. G. Blamire, Phys. Rev. B **61**, 14905(R) (2000).
[47]L. Brey, Phys. Rev. B **75**, 104423 (2007).
[48]R. Rauer, J. Bäckström, D. Budelmann, M. Kurfiß, M. Schilling, M. Rübhausen, T. Walter, K. Dörr, and S. L. Cooper, Appl. Phys. Lett. **81**, 3777 (2002).
[49]A. Tebano *et al*., Phys. Rev. Lett. **100**, 137401 (2008).
[50]B. Holzapfel, B. Roas, L. Schultz, P. Bauer, and G. Saemann-Ischenko, Appl. Phys. Lett. **61**, 3178 (1992).
[51]S. J. May, J. W. Kim, J. M. Rondinelli, E. Karapetrova, N. A. Spaldin, A. Bhattacharya, and P. J. Ryan, Phys. Rev. B **82**, 014110 (2010).
[52]M. C. Dekker, A. D. Rata, K. Boldyreva, S. Oswald, L. Schultz, and K. Dörr, Phys. Rev. B **80**, 144402 (2009).
[53]A. Herklotz, M. D. Biegalski, H.-S. Kim, L. Schultz, K. Dörr, and H. M. Christen, New J. Phys. **12**, 113053 (2010).